Severity of cardiomyopathy associated with adenine nucleotide translocator-1 deficiency correlates with mtDNA haplogroup

Kevin A. Strauss[a,b,c], Lauren DuBiner[b], Mariella Simon[d], Michael Zaragoza[d], Partho P. Sengupta[e], Peng Li[f], Navneet Narula[g], Sandra Dreike[d,h], Julia Platt[d,i], Vincent Procaccio[d,j], Xilma R. Ortiz-González[k], Erik G. Puffenberger[a,b], Richard I. Kelley[l], D. Holmes Morton[a,b,c], Jagat Narula[e], and Douglas C. Wallace[d,k,1]

[a]Clinic for Special Children, Strasburg, PA 17579; [b]Department of Biology, Franklin and Marshall College, Lancaster, PA 17603; [c]Lancaster General Hospital, Lancaster, PA 17602; [d]Departments of Pediatrics and Biological Chemistry and Center for Molecular and Mitochondrial Medicine and Genetics, University of California, Irvine, CA 92697; [e]Mount Sinai Medical Center, New York, NY 10029; [f]Department of Medicine, University of California, Irvine, CA 92697; [g]Department of Pathology, Weill Cornell Medical College, New York, NY 10019; [h]Kapiolani Medical Center for Women and Children, Honolulu, HI 96826; [i]Department of Pediatrics, Stanford University School of Medicine, Palo Alto, CA 94305; [j]Biochemistry and Genetics Department, National Center for Neurodegenerative and Mitochondrial Diseases, Centre Hospitalier Universitaire d' Angers, 49933 Angers, France; [k]Center for Mitochondrial and Epigenomic Medicine, Children's Hospital of Philadelphia and Department of Pathology and Laboratory Medicine, University of Pennsylvania, Philadelphia, PA 19104; and [l]Kennedy Krieger Institute, The Johns Hopkins University School of Medicine, Baltimore, MD 21205

Contributed by Douglas C. Wallace, January 15, 2013 (sent for review December 29, 2012)

Mutations of both nuclear and mitochondrial DNA (mtDNA)–encoded mitochondrial proteins can cause cardiomyopathy associated with mitochondrial dysfunction. Hence, the cardiac phenotype of nuclear DNA mitochondrial mutations might be modulated by mtDNA variation. We studied a 13-generation Mennonite pedigree with autosomal recessive myopathy and cardiomyopathy due to an *SLC25A4* frameshift null mutation (c.523delC, p.Q175RfsX38), which codes for the heart-muscle isoform of the adenine nucleotide translocator–1. Ten homozygous null (adenine nucleotide translocator–$1^{-/-}$) patients monitored over a median of 6 years had a phenotype of progressive myocardial thickening, hyperalaninemia, lactic acidosis, exercise intolerance, and persistent adrenergic activation. Electrocardiography and echocardiography with velocity vector imaging revealed abnormal contractile mechanics, myocardial repolarization abnormalities, and impaired left ventricular relaxation. End-stage heart disease was characterized by massive, symmetric, concentric cardiac hypertrophy; widespread cardiomyocyte degeneration; overabundant and structurally abnormal mitochondria; extensive subendocardial interstitial fibrosis; and marked hypertrophy of arteriolar smooth muscle. Substantial variability in the progression and severity of heart disease segregated with maternal lineage, and sequencing of mtDNA from five maternal lineages revealed two major European haplogroups, U and H. Patients with the haplogroup U mtDNAs had more rapid and severe cardiomyopathy than those with haplogroup H.

ANT1 | oxidative stress | mitochondrial disease | variable penetrance | oxidative phosphorylation

The heart relies on brisk mitochondrial oxidative phosphorylation (OXPHOS) and can preferentially be affected by disorders of mitochondrial energy production (1). Cardiomyopathy associated with OXPHOS dysfunction typically manifests as concentric cardiac enlargement, sometimes beginning in early infancy, and often accompanied by lactic acidosis and progressive multisystem disease (2, 3). Mutations in a number of nuclear DNA (nDNA)–encoded mitochondrial proteins impair OXPHOS and cause cardiomyopathy (4). Recently, two case reports demonstrated homozygous solute carrier family 25, member 4 (*SCL25A4*) (adenine nucleotide translocator–1, *ANT1*) mutations (A123D; c.111+1G > A) (5, 6) in patients who had cardiomyopathy and mitochondrial myopathy without the chronic progressive external ophthalmoplegia (CPEO) characteristic of certain autosomal dominant *ANT1* missense mutations (L98P, A90D, D104G, A114P, and V289M) (7–10).

There are four ANT isoforms in humans; ANT1 is the predominant isoform in heart and skeletal muscle (1, 11). Before the report of ANT1-deficient cardiomyopathy in humans, we inactivated *Slc25a4* to eliminate Ant1 function in a mouse model. This resulted in impaired mitochondrial ADP–ATP exchange, decreased ADP-stimulated tissue respiration, and increased mitochondrial reactive oxygen species (ROS) production in association with cardiomyopathy, mitochondrial myopathy, and lactic acidosis (12, 13). Longitudinal study of $Ant1^{-/-}$ mice indicated that their cardiomyopathy could progress to dilation and heart failure (14). Although mouse extraocular muscles showed mitochondrial pathology, we found no detectable evidence of ophthalmoplegia (15).

Mutations in mtDNA have also been linked to cardiomyopathy (4, 16, 17) and mtDNA mutations have been observed in some patients who have nDNA-encoded sarcomere protein cardiomyopathies (i.e., sarcomeropathies) (18). Both recent deleterious and ancient evolutionarily adaptive mtDNA variants can affect human clinical phenotypes; the latter are associated with region-specific clusters of related mtDNA haplotypes, termed haplogroups (19–21). Haplogroups can differ substantially in their mitochondrial biochemistry, as shown by comparison of cybrids harboring European mtDNA haplogroups H and Uk (22).

In the same year that the first homozygous *SLC25A4* missense mutation was reported (5), we encountered ANT1 deficiency among three Mennonite cousins with cardiomyopathy. We then identified seven additional affected individuals who were part of a larger pedigree segregating an *SLC25A4* frameshift mutation (c.523delC, p.Q175RfsX38), rendering these patients ANT1 null ($ANT1^{-/-}$). Despite shared autozygous (i.e., identical-by-descent) *SLC25A4* mutations and similar environmental exposures among 10 Mennonite patients, the pace and severity of cardiomyopathy were variable and segregated with maternal lineage and mtDNA haplogroup (U versus H).

Results

Molecular Genetics. Ten homozygous $ANT1^{-/-}$ (null) patients were connected across a 13-generation pedigree (Fig. 1*A*). Affymetrix 10,000-marker single nucleotide polymorphism (SNP) genotyping of five affected subjects from three sibships identified a 4.7 Mb block of homozygous SNPs on chromosome 4q35, flanked by SNPs rs1113122 and rs1388935 (Fig. 1*B*). This region contained

Author contributions: D.C.W. designed research; K.A.S., L.D., M.S., M.Z., P.P.S., P.L., N.N., S.D., J.P., V.P., E.G.P., R.I.K., D.H.M., and J.N. performed research; L.D., M.S., M.Z., P.P.S., P.L., N.N., S.D., J.P., V.P., X.R.O.-G., E.G.P., R.I.K., D.H.M., J.N., and D.C.W. analyzed data; and K.A.S., X.R.O.-G., and D.C.W. wrote the paper.

The authors declare no conflict of interest.

Freely available online through the PNAS open access option.

[1]To whom correspondence should be addressed. E-mail: wallaced1@email.chop.edu.

This article contains supporting information online at www.pnas.org/lookup/suppl/doi:10.1073/pnas.1300690110/-/DCSupplemental.

Downloaded at Palestinian Territory, occupied on December 31, 2021

GENETICS

www.manaraa.com

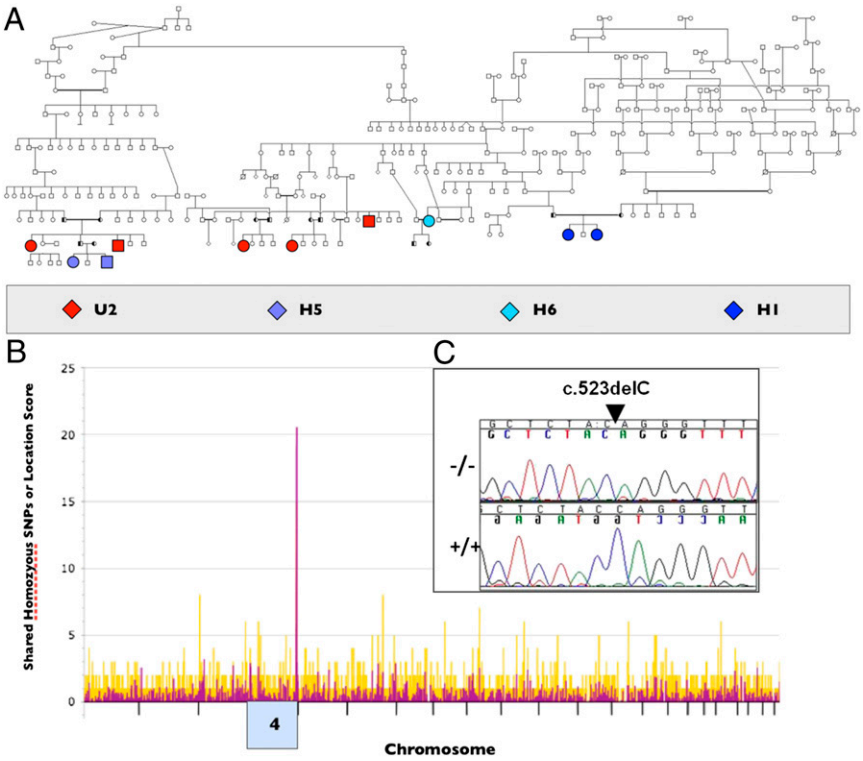

Fig. 1. Extended Mennonite cardiomyopathy pedigree, homozygosity mapping, *ANT1* (*SLC25A4*) frameshift mutant identification, and mtDNA haplogroup determination. (*A*) Genealogical analysis permitted connection of all 10 *ANT1*$^{-/-}$ patients across 13 generations. Among seven affected sibships, there were two haplogroups (H and U) encompassing four different mtDNA subhaplotypes: U2 (red), H5 (violet), H6 (light blue), and H1 (dark blue). (*B*) To map the chromosomal mutant locus, five affected individuals were screened for regions of shared homozygosity using the Affymetrix 10,000-marker SNP genotyping array. Chromosome blocks are separated by downward ticks along the horizontal axis, with chromosome 4 indicated. The vertical axis indicates the number of serial homozygous SNPs shared by all five patients (yellow) or the location score (violet), a calculated value that incorporates population-specific allele frequencies to determine the likelihood that shared blocks are *autozygous*. A single shared 4.7 Mb region on chromosome 4q35, flanked by SNPs rs1113122 and rs1388935, had the highest location score and contained 48 RefSeq genes, including *SLC25A4*. (*C*) Regional sequence of the mutant *ANT1* (*SLC25A4*) gene showing the c.523delC single base deletion that results in a frame shift (p.Q175RfsX38) that destroys the enzyme (Fig. S1*A*).

48 RefSeq genes including *SLC25A4*. Sanger sequencing of *SLC25A4* showed a homozygous single base pair deletion in exon 2 (c.523delC) shared among all affected patients (Fig. 1*C*). The mutation changes codon 175 from glutamine to arginine, prematurely terminates translation at codon 212 (p.Q175RfsX38) (Fig.1*C* and Fig. S1*A*) and removes over a third of the C terminus of the ANT1 polypeptide, which contains several highly conserved amino acids (R234, R235, R236, and E264) critical to the formation of the solute channel (23).

Mitochondrial DNAs from five maternal sibships revealed two European haplogroups, H and U. Haplogroup H mtDNAs comprised subhaplogroups H1, H5, and H6, and haplogroup U mtDNAs belonged to subhaplogroup U2 (Fig. 1*A* and Fig. S1 *B*–*G*).

Clinical Course. Most ANT1$^{-/-}$ infants achieved motor milestones on schedule but were subjectively weaker than their unaffected siblings. Exercise intolerance was first noted during recess activities in the early school years. By later childhood, patients regulated activities to avoid heavy lifting and strenuous exercise. Among adults, even modest exertion (e.g., sweeping the floor) could provoke weakness, dyspnea, and palpitations. Illnesses were often followed by protracted fatigue lasting several days. Cognitive function, academic performance, vision, and hearing were reported normal. However, insomnia and inattention were common, and three of four adult patients suffered from depression and anxiety.

There was no uniform treatment strategy. Eight patients representing both H and U haplogroups were treated with beta-blockers (nadolol, atenolol, metoprolol, or carvedilol), in two cases coupled to an angiotensin II receptor antagonist and in one case coupled to a calcium channel blocker. Two sisters (H1) remained on sustained vitamin-antioxidant therapy (vitamin E, vitamin C, B-complex, coenzyme Q_{10}, and L-carnitine) and received no cardiac medications. Among H haplogroup patients, data were insufficient to determine if mode of treatment (medication versus vitamin-antioxidant therapy) affected disease progression. Among U haplogroup patients, 5 y (range, 2.4–13.3 y) of beta-blocker therapy did not arrest cardiac enlargement (Fig. S2).

Heart Morphology and Performance. ANT1$^{-/-}$ patients were mildly tachycardic and hypertensive (Table 1). Shortening fraction, left ventricular (LV) outflow gradient, and left atrial diameter were normal. Progressive concentric myocardial enlargement began after 3 y of age. All homozygous null patients had longer isovolumic contraction and relaxation times, 40% higher myocardial performance indices (indicating lower myocardial performance), lower estimated cardiac output (mean 2.48 L/m^2 min versus 2.85 L/m^2 min), and shorter mitral valve peak early (E) wave flow velocity deceleration times than normal controls. E velocity and its ratio to the atrial (A) wave flow velocities were normal. Only E velocity correlated with LV mass index among all ANT1$^{-/-}$ patients ($r_s = -0.56$, $P = 0.020$).

Velocity vector imaging (VVI) echocardiography (14) was performed on nine patients; eight patients had radial strains less than 40% of normal, and four of these patients had attenuated longitudinal and circumferential strains (Fig. 2*A*). Mean PR intervals were below average in ANT1 null patients irrespective of age or mitochondrial haplogroup but still within the reference range (Table 1 and Fig. 2 *B* and *C*) (24). As expected, all patients had large R and S wave voltages in precordial leads. Seven of nine

Downloaded at Palestinian Territory, occupied on December 31, 2021
www.manaraa.com

had repolarization abnormalities with inverted T waves in V1 and V6 that could be seen at all ages and in both haplogroups.

Histology. Two ANT1$^{-/-}$, mtDNA haplogroup U patients who were siblings developed end-stage heart failure at ages 15 and 33 y, and their hearts were successfully transplanted. The explanted heart from the 15-y-old male weighed 868 g (510 g/m^2) and was grossly fibrotic along the inner half of the left myocardial wall. LV posterior and interventricular walls were 20 and 28 mm, respectively; the latter impinged on the LV outflow tract. Microscopic

Table 1. Clinical, morphological, functional, and biochemical indices of disease in ANT1 patients and the effect of mitochondrial haplogroup

	Control subjects (n = 28)		All ANT1 patients (n = 9)			ANT1, H haplogroups (n = 5)[§]		ANT1, U2 haplogroup (n = 4)[§]		
Measurements	Mean	SD	Mean	SD	P value*	Mean	SD	Mean	SD	P value*
Age, y	14.0	17.9	14.6	10.6	ns	12.8	12.2	17.6	7.3	ns
Body mass index, kg/m^2	18.3	5.1	18.5	4.0	ns	17.7	3.6	20.0	4.5	ns
Hemodynamics and cardiac morphology										
Systolic blood pressure, mmHg[†]	106.0	9.0	119.0	15.0	0.05	108.0	7.0	129.0	7.0	<0.001
Heart rate, bpm[†]	85.0	11.0	96.0	9.0	0.01	98.0	9.0	93.0	5.0	ns
Left ventricle posterior wall thickness index, diastole, mm/m^2	8.5	2.7	11.8	2.9	0.01	12.0	3.6	11.6	1.1	ns
Interventricular to posterior wall thickness ratio, diastole	1.1	0.3	0.9	0.1	ns	0.9	0.1	1.0	0.2	ns
Left ventricle chamber diameter index, diastole, mm/m^2	38.0	10.9	33.9	10.2	ns	38.6	9.7	26.7	6.2	0.01
Left ventricle wall thickness/chamber diameter ratio, diastole	0.2	0.1	0.4	0.1	0.003	0.3	0.1	0.5	0.1	0.05
Stroke volume index, biplane mode, mL/m^2	33.5	9.8	25.8	7.1	0.02	25.3	6.6	26.6	8.4	ns
Left ventricle mass index, g/m^2	83.0	28.0	141.0	49.0	0.005	114.0	27.0	188.0	42.0	0.006
Left ventricular peak outflow tract gradient, mmHg	4.1	1.9	4.6	2.8	ns	4.0	2.9	5.7	2.4	ns
Left atrial diameter index, systole, mm/m^2	20.0	6.4	20.4	5.7	ns	21.3	6.9	19.4	4.3	ns
Systolic and diastolic function										
Left ventricle shortening fraction, %	39	4	45	6	ns	45	7	46	6	ns
Isovolumic contraction time, ms	28	8	88	13	<0.001	85	12	94	15	ns
Isovolumic relaxation timel ms	38	16	52	13	0.02	49	13	57	15	ns
Myocardial performance (Tei) index	0.28	0.08	0.37	0.08	0.002	0.37	0.06	0.37	0.1	ns
Mitral valve peak E velocity, m/s	0.97	0.12	0.94	0.12	ns	0.99	0.1	0.87	0.13	ns
Mitral valve E/A ratio	1.7	0.8	1.6	0.3	ns	1.6	0.3	1.5	0.1	ns
Deceleration time of E wave, ms	175	45	146	23	0.02	149	25	140	19	ns
Left ventricle wall stress in peak systole (10^3 dynes/cm^2)	142	26	50	18	<0.001	68	39	67	12	ns
Electrocardiogram data[‡]										
PR interval, ms	150	20	114	19	<0.001	112	21	116	18	ns
QRS duration, ms	97	15	95	28	ns	80	11	114	33	ns
Corrected QT interval, ms	411	21	433	40	ns	411	9	461	47	0.05
QRS axis	40	31	66	12	0.009	61	11	75	7	0.008
T wave axis	40	22	−20	39	0.001	−9	44	−39	24	ns
Biochemical indices[¶]										
Creatine kinase, total; IU/L	104	41	98	33	ns	95	20	100	48	ns
Creatine kinase, MB fraction; ng/mL	4.2	1.8	6.5	2.4	ns	5.7	2.6	8.1	1.7	0.04
Troponin I, serum; ng/mL	0.02	0.014	0.066	0.073	ns	0.018	0.01	0.115	0.078	0.03
B-natriuretic peptide, plasma; pg/mL	5	1.7	36	24.2	0.005	33.6	17	58.3	63	ns
Norepinephrine, urine; mcg/g Cr	26	12	114	54	<0.001	110	43	117	56	ns
Total catecholamines, urine; mcg/g Cr	233	48	747	316	0.001	790	355	677	252	ns
Alanine, plasma; μmol/L	440	108	925	351	0.004	969	386	1,188	263	ns
Lactate, plasma; mmol/L	2.1	0.8	7.4	2.2	<0.001	6.9	2.4	8.4	1.5	ns
Lactate/Pyruvate molar ratio (mol:mol)	13	2	34	8	<0.001	34	10	36	2	ns
Lactate/Alanine molar ratio (mol:mol)	5.3	0.7	7.3	1.6	ns	7.6	1.8	6.8	0.9	ns

bpm, beats per minute.

*Unpaired two-tailed t-test using Welch's correction.

[†]To avoid confounding drug effects, statistical testing for blood pressure, heart rate, and urine catecholamines only used data from drug-naïve patients; for mitochondrial haplogroup comparisons, most patients were already being treated with beta blockers.

[‡]Comparison against a subset of 15 control subjects.

[¶]Control groups for comparison, N = 11.

[§]One measurement was obtained for each patient on two different dates separated by a period of 30 mo.

Downloaded at Palestinian Territory, occupied on December 31, 2021
www.manaraa.com

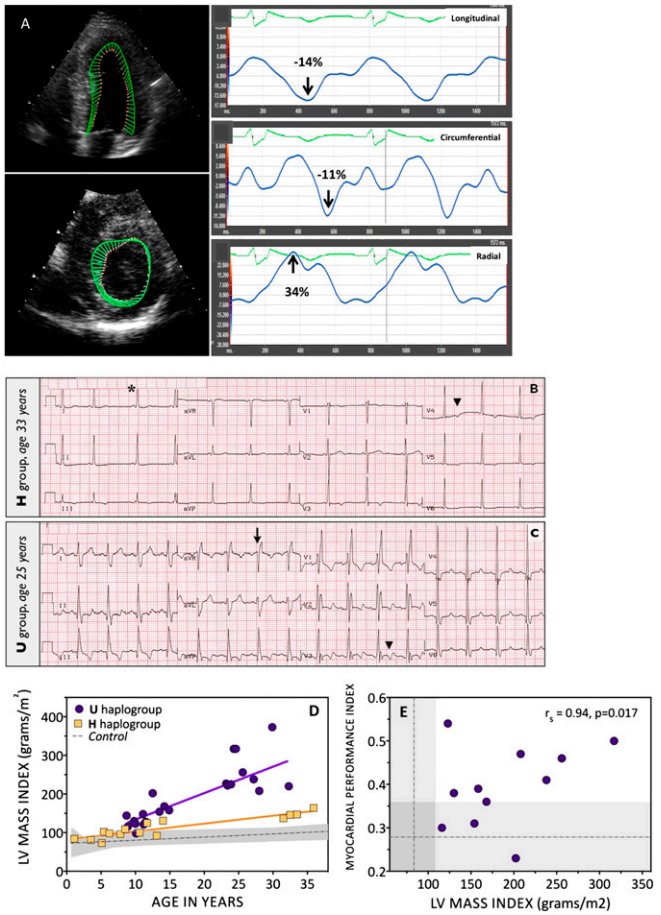

Fig. 2. Cardiac dysfunction of *ANT1* c.523delC mutant patients and the association between mtDNA haplogroup and cardiomyopathy severity and progression. (*A*) VVI echocardiography showing vector analysis of *ANT1*$^{+/+}$ versus *ANT1*$^{-/-}$, mtDNA haplogroup U2 enzyme null heart. VVI tracks the vectorial movement of endocardial borders of the LV in apical, four-chamber, and short axis views for obtaining longitudinal (*Top*), circumferential (*Middle*), and radial (*Bottom*) deformations. LV wall shows concentric hypertrophy with attenuation of peak strains in all three directions reminiscent of comparable data generated for *Ant1*$^{-/-}$ knockout mice (14). (*B* and *C*) Representative electrocardiogram tracings from a 33-y-old woman with H haplogroup mtDNA (*B*) and a 25-y-old man with U haplogroup mtDNA (*C*) show tall R and S wave voltages in precordial leads. Seven of nine ANT1 patients had repolarization abnormalities with inverted T waves in V1 and V6, which could be seen at all ages and in both haplotype groups (arrowheads). Shortened PR intervals were observed (asterisks). Only the two oldest U haplogroup patients had prolonged QRS duration (arrow), in this case showing a right bundle-branch block pattern, whereas QRS duration was normal in younger patients from both mitochondrial haplogroups. (*D*) Cardiac mass index increases progressively in control subjects (gray shaded area, mean ± SD, slope 0.81 ± 0.12, r^2 = 0.92) and homozygous ANT1-deficient patients. Cardiac enlargement is more rapid in patients who have mitochondrial U2 haplogroup (purple circles, slope 3.5 ± 1.4, r^2 = 0.56) versus those with H haplogroups (orange squares, slope 2.1 ± 0.88, r^2 = 0.88); the slopes differ significantly (F = 19.5, $P < 0.0001$). (*E*) There was a strong correlation (r_s = 0.94, P = 0.017) between LV mass index and MPI in affected U haplogroup subjects, suggesting that cardiac energetics declined in parallel with tissue hypertrophy.

examination (Fig. 3 *A–D*) revealed sparse myocytes that were hypertrophic and disoriented, sometimes with markedly enlarged nuclei, evidence of balloon degeneration or frank necrosis. There was extensive interstitial fibrosis, especially in subendocardial regions (Fig. 3*C*). Striking intimal and medial hypertrophy of arteriolar smooth muscle resulted in narrow coronary vessels (arrows in Fig. 3 *B* and *D*).

Electron microscopy (Fig. 3 *E–H*) revealed a decreased number of myofibrils that were irregularly shaped and randomly oriented. Myocytes had abundant, heterogeneous, structurally abnormal mitochondria (Fig. 3 *E* and *F*). Cristae were disfigured and sometimes absent, replaced by vacuolated material or empty space (Fig. 3*G*). Abundant granules in the cytosol most likely represented glycogen. Dark granules of unknown composition were occasionally seen within mitochondria (Fig. 3*H*).

In a skeletal muscle sample, there were many long tubular mitochondria in the subsarcolemmal space but minimal cell necrosis and no interstitial fibrosis. Highly ordered paracrystalline arrays, previously observed in skeletal muscle mitochondria of the two singleton ANT1-deficient patients (5, 6), were not observed.

Physiological Chemistry. Urine norepinephrine and total catecholamines were elevated among ANT1$^{-/-}$ patients (Table 1). Plasma lactate and alanine levels were markedly increased and linearly correlated with each other ($r^2 = 0.58$, $P = 0.01$). The ratio of lactate to pyruvate in blood was elevated two- to threefold, providing indirect evidence of a highly reduced respiratory chain and elevated NADH–NAD$^+$ ratio. Markers of myocyte injury did not differ between patients and controls, but B-natriuretic peptide was elevated sevenfold in the ANT1$^{-/-}$ patients ($P = 0.005$).

Variable Clinical Course and Relation to Mitochondrial Haplogroup. Mitochondrial haplogroup H and U ANT1$^{-/-}$ patients experienced similar symptoms, but mtDNA haplogroup U patients had more rapidly progressive and severe heart disease (Table 1 and Fig. 2*D*). At the extreme, one haplogroup U patient required a heart transplant for intractable heart failure at 15 y of age. His haplogroup U sister had a septal myomectomy during late adolescence because of fatigue, presyncopal events, and massive concentric cardiac enlargement (LV mass 373 g/m^2) and subsequently developed heart failure and was transplanted at age 33 y.

Cardiac enlargement progressed 67% faster in association with U versus H haplogroups (Fig. 2*D*). Restricting analyses to U haplogroup revealed strong correlations of LV mass index to both the E–A ratio (r_s = 0.89, P = 0.033) and myocardial performance index (MPI) (r_s = 0.94, P = 0.017; Fig. 2*E*). EKG abnormalities (Fig. 2 *B* and *C*) included inverted T waves and prominent R and S waves in precordial leads. Prolonged QRS duration (148 and 136 ms) was found in the two oldest U haplogroup patients (one showing a right bundle-branch block). Both of these haplogroup U subjects had a long QTc interval (up to 521 ms). Creatine kinase MB (cardiac isoform) fraction and troponin I were 40% and sixfold higher, respectively, in U versus H haplogroup ANT1$^{-/-}$ patients (Table 1).

Discussion

Clinical analysis of nine related ANT1$^{-/-}$ patients has confirmed that complete absence of ANT1 activity in humans is associated with lactic academia, cardiomyopathy, and mitochondrial myopathy without CPEO, consistent with previous case reports (5, 6). Therefore, ANT1$^{-/-}$ disease is clinically and presumably functionally distinct from the familial dominant negative ANT1 disease (7–10).

Despite autozygosity for *SLC25A4* c.523delC and similar environmental exposures among all affected Mennonite patients, we observed significant clinical variability among the ANT1$^{-/-}$ patients. Although this variability could result for segregating nDNA modifier genes, we noticed that the greatest phenotypic variability appeared to segregate with maternal lineage. Sequencing mtDNA from these lineages revealed an association of mtDNA haplogroup U with more severe cardiomyocyte injury and tissue remodeling. Indeed, the only two ANT1$^{-/-}$ patients who required heart transplantation were siblings with mtDNA haplogroup U2e1, whereas all mtDNA haplogroup H patients had comparatively mild heart disease.

The putative association between cardiomyopathy severity and mtDNA haplogroup is consistent with observations from human somatic cybrid cell lines expressing H and Uk mtDNAs. Compared

Downloaded at Palestinian Territory, occupied on December 31, 2021
www.manaraa.com

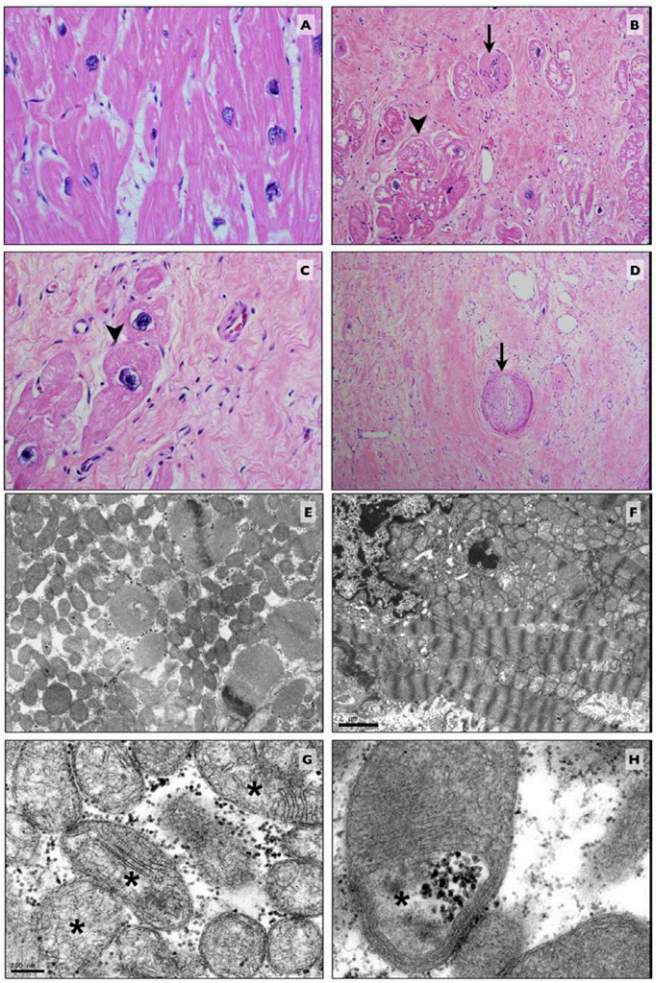

Fig. 3. Myocardial histopathology of explanted heart from a 15-y-old *ANT1*$^{-/-}$, haplogroup U2, patient showing severe cardiomyocyte and mitochondrial abnormalities. The explanted *ANT1*$^{-/-}$, haplogroup U heart weighed 868 g (510 g/m^2) with left posterior and interventricular septal walls measuring 20 and 28 mm, respectively. (*A–D*) Ventricle sections stained with H&E and examined by light microscopy and (*E* and *F*) ventricle sections examined by electron microscopy. (*A*) In areas of relative myocardial sparing, fiber orientation was distorted. (*B* and *C*) In most LV regions, myocytes were sparse, hypertrophic, and disoriented (sometimes with markedly enlarged nuclei) and showed evidence of balloon degeneration or frank necrosis (arrowheads). (*D*) There was extensive interstitial fibrosis, especially in subendocardial regions, where myocytes were almost completely replaced by connective tissue. Striking intimal and medial hypertrophy of arteriolar smooth muscle (arrow) resulted in narrow coronary vessels. (*E* and *F*) High mitochondrial density together with a paucity of myofibrils that are irregularly shaped and disoriented. (*G*) Cristae disfiguration and regions of empty mitochondria devoid of cristae (asterisks). (*H*) Dark granules of unclear composition occasionally seen within mitochondria.

with H cybrids, Uk cybrids have less mtDNA, mitochondrial rRNA, total mitochondrial protein, and complex IV activity (22). U2 mitochondria are not biochemically identical to Uk, but are still likely impaired relative to haplogroup H mitochondria. Subhaplogroups Uk and U2 share haplogroup U founder variants tRNA$^{Leu(CUN)}$ A12308G and 16S rRNA A118G, but also have distinct differences: U2 has a tRNA^{Thr} T15907C variant, whereas Uk has ATP6 G9055A (A177T) and cytochrome *b* T14798C (F18L) variants (25). Haplogroup U mitochondria that harbor the A12308G and A118G variants are associated with reduced sperm motility (26) and more alkaline postmortem brain tissue (27), confirming biologically relevant functional differences between haplogroup U and H mtDNAs. The functional consequences of polymorphic mtDNA are also evident in cybrid cell lines, where both single mtDNA polypeptide changes and mtDNA haplogroup variation can give rise to 25–30% differences in complex I activity (21). Available evidence from humans suggests that disease phenotype caused by nDNA mutations can be modified by mtDNA variation. This has been studied in cardiomyopathy patients who co-inherit nDNA contractile protein and mtDNA mutations (18), and in the pathological interaction between a mild X-linked complex I gene *NDUFA1* variant and a pair of nonpathogenic mtDNA complex I polypeptide missense mutations (28).

The pathology of ANT1$^{-/-}$ cardiomyopathy is similar to other forms of end-stage hypertrophic cardiomyopathy caused by sarcomeric protein mutations (29, 30). Common clinical features include concentric myocardial wall thickening, tachycardia, short PR interval, typical electrocardiogram (EKG) changes, progressive fibrosis, and end-stage chamber dilation. However, there are features of ANT1$^{-/-}$ disease that distinguish it from the more common sarcomeropathies. These include congenital muscle weakness, subsarcolemmal mitochondrial proliferation, highly symmetric wall thickening, and marked elevations of lactate and alanine. Comorbid insomnia and depression in ANT1$^{-/-}$ patients could result in part from persistent adrenergic activation (as indicated by high urine catecholamines, tachycardia, hypertension, and short PR interval), which has been associated with insomnia (31), depression (32, 33), and anxiety (32, 34) in other clinical contexts.

The pathophysiology of ANT1$^{-/-}$ cardiomyopathy can likely be traced to multiple interacting functions of mitochondrial OXPHOS, such as energy production, control of cellular redox status, generation of cellular ROS, control of cytosolic calcium, initiation of the intrinsic apoptotic cell death, and modulation of the flow of metabolic intermediates (1, 35). Insight into the pathophysiology can be gleaned from Ant1 null mice, which closely parallel the mitochondrial and cardiac phenotype of Mennonite patients and have similar contractile abnormalities on echocardiographic VVI (12, 14). Mitochondria of Ant1$^{-/-}$ mice have markedly reduced ADP-stimulated respiration rates, most apparent in the skeletal muscle mitochondria that rely almost exclusively on ANT1 as an ADP/ATP translocator and show a massive induction of mitochondrial proliferation and a down-regulation of glycolysis, presumably as a futile attempt to compensate for the diminished mitochondrial ATP export (36, 37). Reduced single mitochondrion ATP flux limits sarcomere contraction and also entrains marked compensatory proliferation of cardiac mitochondria, but the adapted myocardium continues to contract inefficiently and dyssynchronously.

Inhibition of ATP–ADP exchange inhibits the ATP synthase, and the resulting increased mitochondrial membrane potential slows electron flux through the electron transport chain with the result that the respiratory chain enzymes become saturated with electrons. This raises the mitochondrial ratio of NADH to NAD$^+$, inhibiting the tricarboxylic acid cycle, and resulting in the accumulation of pyruvate and NADH in cytosol that drives lactic acidosis (12, 38). The high electron density of the respiratory chain enzymes also increases single electron transfer to O_2, resulting in elevated mitochondrial ROS production (1, 13, 36, 39, 40). The resulting oxidative damage causes the accumulation of mtDNA mutations including the rearrangements documented in both ANT1$^{-/-}$ and ANT1$^{+/-}$ patients and Ant1$^{-/-}$ mice (5–10, 13). The sum of these various factors ultimately leads to cardiomyocyte demise.

Finally, neither beta-blocker nor antioxidant-vitamin therapy appear to influence the natural progression of ANT1$^{-/-}$ heart disease, but more potent antioxidant (41) or antifibrotic therapies (42–44) might prove effective. We are currently investigating replacement of ANT1 function by adeno-associated virus gene therapy as a means to more decisively prevent the progression of ANT1$^{-/-}$ disease (36).

Downloaded at Palestinian Territory, occupied on December 31, 2021
www.manaraa.com

Patients and Methods

This study was approved by the Institutional Review Boards of Lancaster General Hospital and the University of California, Irvine. Adult patients consented in writing to participate and parents consented for their children. Ten patients of Northeastern Mennonite ancestry were studied. One had a cardiac transplant before molecular diagnosis; thus, nine (age, 14.6 ± 10.6 y; range, 1–36 y; seven female) were available for detailed longitudinal studies. Standard histological sections and electron micrographs were examined from the explanted heart and a single skeletal muscle biopsy.

We used five affected children from four sibships to scan 10K-marker SNP genotypes (Affymetrix) for regions of autozygosity (identity-by-descent) (45) and sequenced target genes by the Sanger method (46). mtDNA sequencing and haplogroup assignment were performed as previously described (25, 47) and reported as differences from the revised Cambridge Reference Sequence (48). Clinical data were collected during routine office visits over a median of 6 (range, 4–16) y, but we restricted statistical analyses for Table 1 to values obtained on two separate days (2008 and 2011) spaced 30 mo apart. Clinical data collection by ultrasound, electrocardiographic, and physiological chemical methods are detailed in *SI Patients and Methods*.

ACKNOWLEDGMENTS. The authors deeply appreciate the assistance of Ms. Marie Lott for preparation of this manuscript. This work was supported by Postdoctoral Fellowship 5T32NS007413-14 (to X.R.O.-G.) and National Institutes of Health R01 Grants NS41850, NS21328, and DK73691 (to D.C.W.).

1. Wallace DC (2005) A mitochondrial paradigm of metabolic and degenerative diseases, aging, and cancer: A dawn for evolutionary medicine. *Annu Rev Genet* 39:359–407.
2. Nishizawa M, et al. (1987) A mitochondrial encephalomyopathy with cardiomyopathy. A case revealing a defect of complex I in the respiratory chain. *J Neurol Sci* 78(2): 189–201.
3. Guenthard J, Wyler F, Fowler B, Baumgartner R (1995) Cardiomyopathy in respiratory chain disorders. *Arch Dis Child* 72(3):223–226.
4. Wallace DC, Lott MT, Procaccio V (2013) *Emery and Rimoin's Principles and Practice of Medical Genetics, Mitochondrial Medicine: The Mitochondrial Biology and Genetics of Metabolic and Degenerative Diseases, Cancer, and Aging*, Chapter 13, eds Rimoin DL, Pyeritz RE, Korf BR (Churchill Livingstone Elsevier, Philadelphia), 6th Ed, Vol 1.
5. Palmieri L, et al. (2005) Complete loss-of-function of the heart/muscle-specific adenine nucleotide translocator is associated with mitochondrial myopathy and cardiomyopathy. *Hum Mol Genet* 14(20):3079–3088.
6. Echaniz-Laguna A, et al. (2012) Complete loss of expression of the ANT1 gene causing cardiomyopathy and myopathy. *J Med Genet* 49(2):146–150.
7. Kaukonen J, et al. (2000) Role of adenine nucleotide translocator 1 in mtDNA maintenance. *Science* 289(5480):782–785.
8. Chen XJ (2002) Induction of an unregulated channel by mutations in adenine nucleotide translocase suggests an explanation for human ophthalmoplegia. *Hum Mol Genet* 11(16):1835–1843.
9. De Marcos Lousa C, et al. (2005) Valine 181 is critical for the nucleotide exchange activity of human mitochondrial ADP/ATP carriers in yeast. *Biochemistry* 44(11): 4342–4348.
10. De Marcos Lousa C, Trézéguet V, Dianoux AC, Brandolin G, Lauquin GJ (2002) The human mitochondrial ADP/ATP carriers: Kinetic properties and biogenesis of wild-type and mutant proteins in the yeast S. cerevisiae. *Biochemistry* 41(48):14412–14420.
11. Stepien G, Torroni A, Chung AB, Hodge JA, Wallace DC (1992) Differential expression of adenine nucleotide translocator isoforms in mammalian tissues and during muscle cell differentiation. *J Biol Chem* 267(21):14592–14597.
12. Graham BH, et al. (1997) A mouse model for mitochondrial myopathy and cardiomyopathy resulting from a deficiency in the heart/muscle isoform of the adenine nucleotide translocator. *Nat Genet* 16(3):226–234.
13. Esposito LA, Melov S, Panov A, Cottrell BA, Wallace DC (1999) Mitochondrial disease in mouse results in increased oxidative stress. *Proc Natl Acad Sci USA* 96(9):4820–4825.
14. Narula N, et al. (2011) Adenine nucleotide translocase 1 deficiency results in dilated cardiomyopathy with defects in myocardial mechanics, histopathological alterations, and activation of apoptosis. *JACC Cardiovasc Imaging* 4(1):1–10.
15. Yin H, et al. (2005) Eliminating the Ant1 isoform produces a mouse with CPEO pathology but normal ocular motility. *Invest Ophthalmol Vis Sci* 46(12):4555–4562.
16. Arbustini E, et al. (1998) Mitochondrial DNA mutations and mitochondrial abnormalities in dilated cardiomyopathy. *Am J Pathol* 153(5):1501–1510.
17. Zaragoza MV, Brandon MC, Diegoli M, Arbustini E, Wallace DC (2011) Mitochondrial cardiomyopathies: How to identify candidate pathogenic mutations by mitochondrial DNA sequencing, MITOMASTER and phylogeny. *Eur J Hum Genet* 19(2):200–207.
18. Arbustini E, et al. (1998) Coexistence of mitochondrial DNA and beta myosin heavy chain mutations in hypertrophic cardiomyopathy with late congestive heart failure. *Heart* 80(6):548–558.
19. Ruiz-Pesini E, Mishmar D, Brandon M, Procaccio V, Wallace DC (2004) Effects of purifying and adaptive selection on regional variation in human mtDNA. *Science* 303(5655):223–226.
20. Ruiz-Pesini E, Wallace DC (2006) Evidence for adaptive selection acting on the tRNA and rRNA genes of human mitochondrial DNA. *Hum Mutat* 27(11):1072–1081.
21. Ji F, et al. (2012) Mitochondrial DNA variant associated with Leber hereditary optic neuropathy and high-altitude Tibetans. *Proc Natl Acad Sci USA* 109(19):7391–7396.
22. Gómez-Durán A, et al. (2010) Unmasking the causes of multifactorial disorders: OXPHOS differences between mitochondrial haplogroups. *Hum Mol Genet* 19(17): 3343–3353.
23. Pebay-Peyroula E, et al. (2003) Structure of mitochondrial ADP/ATP carrier in complex with carboxyatractyloside. *Nature* 426(6962):39–44.
24. Sharieff GQ, Rao SO (2006) The pediatric ECG. *Emerg Med Clin North Am* 24(1): 195–vii–208viii.
25. Ruiz-Pesini E, et al. (2007) An enhanced MITOMAP with a global mtDNA mutational phylogeny. *Nucleic Acids Res* 35(Database issue):D823–D828.
26. Montiel-Sosa F, et al. (2006) Differences of sperm motility in mitochondrial DNA haplogroup U sublineages. *Gene* 368:21–27.
27. Rollins B, et al. (2009) Mitochondrial variants in schizophrenia, bipolar disorder, and major depressive disorder. *PLoS ONE* 4(3):e4913.
28. Potluri P, et al. (2009) A novel NDUFA1 mutation leads to a progressive mitochondrial complex I-specific neurodegenerative disease. *Mol Genet Metab* 96(4):189–195.
29. Elliott P, McKenna WJ (2004) Hypertrophic cardiomyopathy. *Lancet* 363(9424): 1881–1891.
30. Maron BJ (2002) Hypertrophic cardiomyopathy: A systematic review. *JAMA* 287(10): 1308–1320.
31. Mitchell HA, Weinshenker D (2010) Good night and good luck: Norepinephrine in sleep pharmacology. *Biochem Pharmacol* 79(6):801–809.
32. Boulenger JP, Uhde TW (1982) Biological peripheral correlates of anxiety. *Encephale* 8(2):119–130.
33. Oei TP, Dingle GA, McCarthy M (2010) Urinary catecholamine levels and response to group cognitive behaviour therapy in depression. *Behav Cogn Psychother* 38(4): 479–483.
34. Pervanidou P, Chrousos GP (2010) Neuroendocrinology of post-traumatic stress disorder. *Prog Brain Res* 182:149–160.
35. Wallace DC (2012) Mitochondria and cancer. *Nat Rev Cancer* 12(10):685–698.
36. Murdock DG, Boone BE, Esposito LA, Wallace DC (1999) Up-regulation of nuclear and mitochondrial genes in the skeletal muscle of mice lacking the heart/muscle isoform of the adenine nucleotide translocator. *J Biol Chem* 274(20):14429–14433.
37. Subramaniam V, et al. (2008) MITOCHIP assessment of differential gene expression in the skeletal muscle of Ant1 knockout mice: Coordinate regulation of OXPHOS, antioxidant, and apoptotic genes. *Biochim Biophys Acta* 1777(7-8):666–675.
38. Flierl A, Chen Y, Coskun PE, Samulski RJ, Wallace DC (2005) Adeno-associated virus-mediated gene transfer of the heart/muscle adenine nucleotide translocator (ANT) in mouse. *Gene Ther* 12(7):570–578.
39. Pryde KR, Hirst J (2011) Superoxide is produced by the reduced flavin in mitochondrial complex I: A single, unified mechanism that applies during both forward and reverse electron transfer. *J Biol Chem* 286(20):18056–18065.
40. Lombardi R, et al. (2009) Resolution of established cardiac hypertrophy and fibrosis and prevention of systolic dysfunction in a transgenic rabbit model of human cardiomyopathy through thiol-sensitive mechanisms. *Circulation* 119(10):1398–1407.
41. Wallace DC, Fan W, Procaccio V (2010) Mitochondrial energetics and therapeutics. *Annu Rev Pathol* 5:297–348.
42. Cacciapuoti F (2011) Molecular mechanisms of left ventricular hypertrophy (LVH) in systemic hypertension (SH)-possible therapeutic perspectives. *J Am Soc Hypertens* 5(6):449–455.
43. Kuster GM, et al. (2005) Alpha-adrenergic receptor-stimulated hypertrophy in adult rat ventricular myocytes is mediated via thioredoxin-1-sensitive oxidative modification of thiols on Ras. *Circulation* 111(9):1192–1198.
44. Teekakirikul P, et al. (2010) Cardiac fibrosis in mice with hypertrophic cardiomyopathy is mediated by non-myocyte proliferation and requires Tgf-β. *J Clin Invest* 120(10): 3520–3529.
45. Strauss KA, Puffenberger EG (2009) Genetics, medicine, and the Plain people. *Annu Rev Genomics Hum Genet* 10:513–536.
46. Puffenberger EG, et al. (2004) Mapping of sudden infant death with dysgenesis of the testes syndrome (SIDDT) by a SNP genome scan and identification of TSPYL loss of function. *Proc Natl Acad Sci USA* 101(32):11689–11694.
47. Poole JC, Procaccio V, Brandon MC, Merrick G, Wallace DC (2010) Multiplex analysis of mitochondrial DNA pathogenic and polymorphic sequence variants. *Biol Chem* 391(10):1115–1130.
48. Andrews RM, et al. (1999) Reanalysis and revision of the Cambridge reference sequence for human mitochondrial DNA. *Nat Genet* 23(2):147.

Downloaded at Palestinian Territory, occupied on December 31, 2021

www.manaraa.com